Biochemistry and Biophysics Reports 7 (2016) 379–385

Contents lists available at ScienceDirect

Biochemistry and Biophysics Reports

journal homepage: www.elsevier.com/locate/bbrep

Identification of the *agg1* mutation responsible for negative phototaxis in a "wild-type" strain of *Chlamydomonas reinhardtii*

Takahiro Ide [a,1], Shota Mochiji [b], Noriko Ueki [a,c], Katsushi Yamaguchi [d], Shuji Shigenobu [d,e], Masafumi Hirono [f], Ken-ichi Wakabayashi [a,*]

[a] Laboratory for Chemistry and Life Science, Institute of Innovative Research, Tokyo Institute of Technology, Yokohama 226-8503, Japan
[b] Department of Biological Sciences, Graduate School of Science, University of Tokyo, Tokyo 113-0033, Japan
[c] Department of Biological Sciences, Graduate School of Science and Engineering, Chuo University, Tokyo 112-8551, Japan
[d] Functional Genomics Facility, National Institute for Basic Biology, Okazaki, Aichi 444-8585, Japan
[e] Department of Basic Biology, Faculty of Life Science, SOKENDAI (The Graduate University for Advanced Studies), Okazaki, Aichi 444-8585, Japan
[f] Department of Frontier Bioscience, Hosei University, Tokyo 184-8584, Japan

ARTICLE INFO

Article history:
Received 4 April 2016
Received in revised form
22 June 2016
Accepted 18 July 2016
Available online 20 July 2016

Keywords:
Chlamydomonas
Phototaxis
Next-generation sequence

ABSTRACT

The unicellular green alga *Chlamydomonas reinhardtii* is a model organism for various studies in biology. CC-124 is a laboratory strain widely used as a wild type. However, this strain is known to carry *agg1* mutation, which causes cells to swim away from the light source (negative phototaxis), in contrast to the cells of other wild-type strains, which swim toward the light source (positive phototaxis). Here we identified the causative gene of *agg1* (*AGG1*) using AFLP-based gene mapping and whole genome next-generation sequencing. This gene encodes a 36-kDa protein containing a Fibronectin type III domain and a CHORD-Sgt1 (CS) domain. The gene product is localized to the cell body and not to flagella or basal body.

1. Introduction

The biflagellated unicellular green alga *Chlamydomonas reinhardtii* is a model organism used in various fields of biology, such as flagellar motility, photosynthesis, photomovement and sexual reproduction. One of its strong advantages is the feasibility of genetic studies. *C. reinhardtii* has two mating types (mt+ and mt−) and undergoes sexual reproduction under nitrogen-starved conditions, which results in the production of four daughter cells amenable to classical tetrad analysis.

Among several wild-type strains of *C. reinhardtii*, the most widely used are CC-125 (mt+) and CC-124 (mt−). This pair has descended from Ebersold/Levine 137c strain, from which many mutants have been isolated [1]. However, strictly speaking, CC-125 and CC-124 are mutants: both carry mutations in *NIT1* and *NIT2* loci and cannot grow on nitrate as the sole nitrogen source [1,2]. Moreover, CC-124, but not CC-125, carries a mutation in the *AGG1* locus, which causes strong negative phototaxis; cells form aggregates at the bottom of a test tube under room light, in contrast to the positively phototactic CC-125 tending to swim toward the surface of the medium [3]. Hereinafter we refer to CC-124 as *agg1*.

Since the *agg1* mutant has been used as a wild type, the mutation in the *AGG1* locus must be unintentionally present in many mutant strains [1]. The sign of phototaxis is regulated by various cellular factors, such as the phase of circadian rhythm, reduction-oxidation poise and internal cAMP level [4–6]. In order to precisely understand the phenotypes of mutants deficient in the phototactic signaling pathway, we need to determine the presence or absence of *agg1* in experimental strains. Identification of the *AGG1* gene is therefore important for studies using *C. reinhardtii* and related green algae, particularly in the field of photobiology and behavior. Classical genetic studies based on tetrad analysis have mapped the *AGG1* locus to linkage group XIV (currently chromosome 13) [3]. However, the locus has not been sufficiently narrowed down to allow determination of the causative gene.

In this study, we identified the *agg1* mutation by AFLP-based gene mapping and next-generation sequencing. The causative gene encodes a novel protein containing a Fibronectin type III domain and a CHORD-Sgt1(CS) domain. This protein was found localized to the cell body and not to the flagella.

2. Materials and methods

2.1. Strains and culture of *Chlamydomonas reinhardtii*

Chlamydomonas reinhardtii strains, CC-125 (*AGG1*; mt+) and CC-124 (*agg1*; mt−), were obtained from the *Chlamydomonas*

* Corresponding author.
E-mail address: wakaba@res.titech.ac.jp (K.-i. Wakabayashi).
[1] Present address: Laboratory for Organismal Patterning, RIKEN Center for Developmental Biology, Kobe, Hyogo 650-0047, Japan.

http://dx.doi.org/10.1016/j.bbrep.2016.07.016

Center (http://www.chlamy.org/). These strains and the transformants *agg1*::AGG1-3 × hemagglutinin (HA) and *bld12*::SAS6-HA were grown in Tris-acetate-phosphate (TAP) medium with aeration at 25 °C on a 12 h/12 h light/dark cycle [7,8]. For immunofluorescence microscopy, cells were grown under constant illumination.

2.2. Linkage mapping of AGG1

CC-125 was crossed to *agg1* (mt−) to obtain an *agg1* (mt+) strain. The *agg1* (mt+) strain was crossed to a polymorphic strain, S1C5 (mt−, CC-1952; [9]), for AFLP-based gene mapping. Recombination frequencies between *agg1* and genetic markers were determined by detecting polymorphic PCR products in 77 progenies that displayed strong negative phototaxis [10]. The *agg1* mutation was mapped to a 1537-kb region between two genetic markers on chromosome 13: STS79-178 (5′-TAGGGACACCCAAGGTAATGAGCA-3′, 5′-ACGCTCAACTGTTCTAGACCCGAG-3′ and 5′-CCGGAAGGCTAC-GAATGAGATACA-3′) and SSR116–16 (5′-CTCGGGTGAGCTGCAAT-CAGTAG-3′ and 5′-CCTGTAAGCCCAGACAGGTCAAAC-3′).

2.3. Whole genome sequencing

Cell walls were removed from cells of *agg1* and *AGG1* (selected from the progenies of an *agg1* × CC-125 cross) strains by autolysin treatment [1]. DNA was prepared using a DNeasy Plant Mini kit (QIAGEN) following the manufacturer's instructions. Two micrograms of each DNA sample was fragmented using a Covaris sonicator. ~300 bp DNA fragments were then purified using a Pippin Prep system (Sage Science) and were used to construct sequence libraries using an Illumina TruSeq library prep kit (Illumina) essentially following the manufacturer's instruction except that the number of PCR cycles in the amplification enrichment step was reduced to six to minimize the PCR amplification bias. The libraries were sequenced using Illumina HiSeq 2000 to produce 2 × 101 bp paired-end reads. In total, 48.2 M (9.7 Gbp) and 71.6 M paired-end reads (14.5 Gbp) were obtained for *agg1* and the *AGG1* strain, respectively.

Sequence reads were aligned onto the Joint Genome Institute (JGI) version 5.3.1 (Creinhardtii_236.fa.gz) *Chlamydomonas* genome sequence (https://phytozome.jgi.doe.gov/pz/portal.html#! info?alias=Org_Creinhardtii) using bowtie2 (http://bowtie-bio.sourceforge.net/bowtie2/index.shtml). The resulting SAM (Sequence Alignment/Map) files were converted to BAM (Binary Sequence Alignment/Map) and sorted by SAMtools version 0.1.18 (http://samtools.sourceforge.net/). To identify the mutation in the mapped region of *agg1* genome, the alignment data were visualized using IGV software (version 2.3.39; https://www.broadinstitute.org/igv/) and compared to each other or to the genome database.

2.4. PCR for AGG1 cloning and detection of transposon X56231.1

For cloning of *AGG1* cDNA, total RNA was prepared and reverse-transcription PCR was performed following the method of [11], using primers 5′-GCGCCATATGTCCTGGCTCAGCAGCTTT-3′ and 5′-GCGCAGATCTTCAATCCCAGCTGGGCCGG-3′.

For detection of transposon insertion at 5′ untranslated region (UTR) of *AGG1*, the following primers were used: #1: 5′-CTAACG-CAACACGGCAGTTA-3′, #2: 5′-CCTGCATTGAGACTGCGCCC-3′, #3:5′-TTAGGGCCAGTGGTGGTTTA-3′ (see Fig. 1C for details).

2.5. Generation of anti-AGG1 antibody

AGG1 cDNA with a 6 × His tag at the C terminus was cloned into a bacterial expression vector, pMaL-c2X (New England Biolabs). AGG1 was expressed as a fusion protein with maltose-binding protein (MBP). MBP-AGG1-6 × His was purified using amylose resin (New England Biolabs) and used to immunize a guinea pig. The obtained antiserum was blot-purified using AGG1 after proteolytic removal of MBP- and 6 × His-tags.

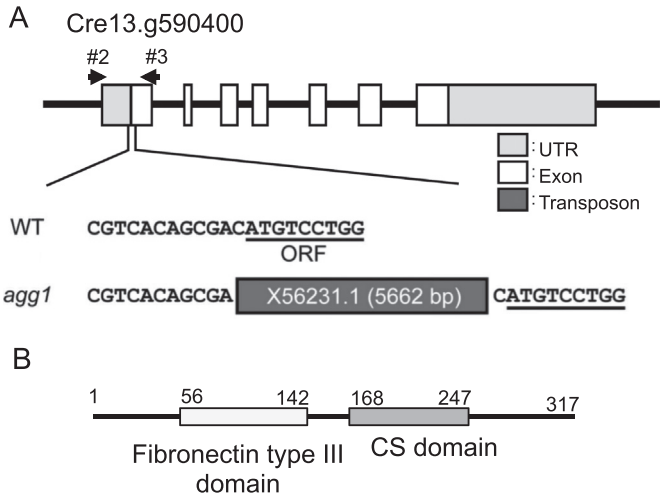

Fig. 1. Identification of *AGG1* as Cre13.g590400. (A) The gene structure. A transposon X5623.1 is inserted in the 5′ UTR of Cre13.g590400 in the *agg1* mutant. Arrows indicate the position of primers designed to detect the transposon insertion (#1~#3; see Fig. 2). (B) Domain structures of the predicted product.

2.6. Generation of agg1::AGG1–3 × HA strain

The cDNA of *AGG1* with a 3 × HA tag at the C terminus was cloned into the pGenD expression vector containing the paromomycin resistance gene *aphVIII* [12,13]. The DNA construct was introduced into *agg1* cells by electroporation (NEPAGENE) [14]. A transformant that displayed positive phototaxis and expressed AGG1-3 × HA was isolated.

2.7. Phototaxis assay

Dish phototaxis assay was performed following the method of [5]. Tube phototaxis assay was performed following the method of [3] with modifications. Briefly, cells were washed with an assay solution (5 mM Hepes (pH 7.4), 0.2 mM EGTA, 1 mM KCl, and 0.3 mM $CaCl_2$) and kept under red light for ~1 h before the assays. Cell suspensions (~7 ml, ~1×10^7 cells/ml) were put in test tubes (18 mm × 180 mm) and illuminated with a white LED (ATTO Flatviewer; ATTO) from the top. Cell distribution patterns in both assays were photographed.

2.8. Fluorescence microscopy

Immunofluorescence microscopy was carried out as described previously [15]. Anti-HA tag antibody (1:200, 11867423001; Roche Applied Science) and anti-acetylated α-tubulin antibody (1:200, ab24610; abcam) were used as primary antibodies. Anti-mouse IgG antibody conjugated with Alexa Fluor 350 (1:200, A11045; Life technologies) and anti-rat IgG antibody conjugated with DyLight 549 (1:200, 612-142-120; ROCKLAND) were used as secondary antibodies. Images were taken with a CCD camera (DP73; Olympus).

2.9. Western blot analysis

Western blot analysis of cell fractions was carried out using anti-HA (11867423001; Roche Applied Science) and anti-ODA-IC2 (D6168; Sigma Aldrich) antibodies as primary antibodies and anti-rat IgG (NA935V; GE Health Care), anti-mouse IgG (NA931V; GE

Health Care), and anti-guinea pig IgG (A7289; Sigma-Aldrich) antibodies as secondary antibodies. The cell fractions were prepared following the procedures described previously [16].

3. Results

3.1. Identification of AGG1 by linkage mapping and next-generation sequencing

The *AGG1* locus was narrowed down to an ~1537-kb region on chromosome 13 by linkage mapping (see Section 2). The causal mutation of *agg1* was searched for in the mapped region by a visual comparison of genome sequence of the *agg1* mutant with that of an *agg1*-free progeny from the cross *agg1* × CC-125 or with that of the strain CC-503 registered in the JGI database using the IGV browser (see Section 2). We found three *agg1*-specific mutations in the mapped region: in Cre13.g590400, paired-reads of the *agg1* genome did not exactly map to the 5′ terminus of the first exon in the reference database, suggesting an insertion; Cre13.g603000t2.1 and Cre13.g604250 have a single nucleotide substitution in an intron (13:4,387,946 bp C to A, and 13:4,655,586 bp G to A, respectively). Among these, the mutation in the Cre13.g590400 is the most likely candidate. Sanger DNA sequencing of this locus revealed that an insertion of a transposon, X56231.1 (also known as TOC1) in the 5′ UTR of Cre13.g590400 [17,18] (Fig. 1A). It is a non-autonomous version of TOC3, a retroelement encoding a tyrosine recombinase, widespread in the *C. reinhardtii* genome [19].

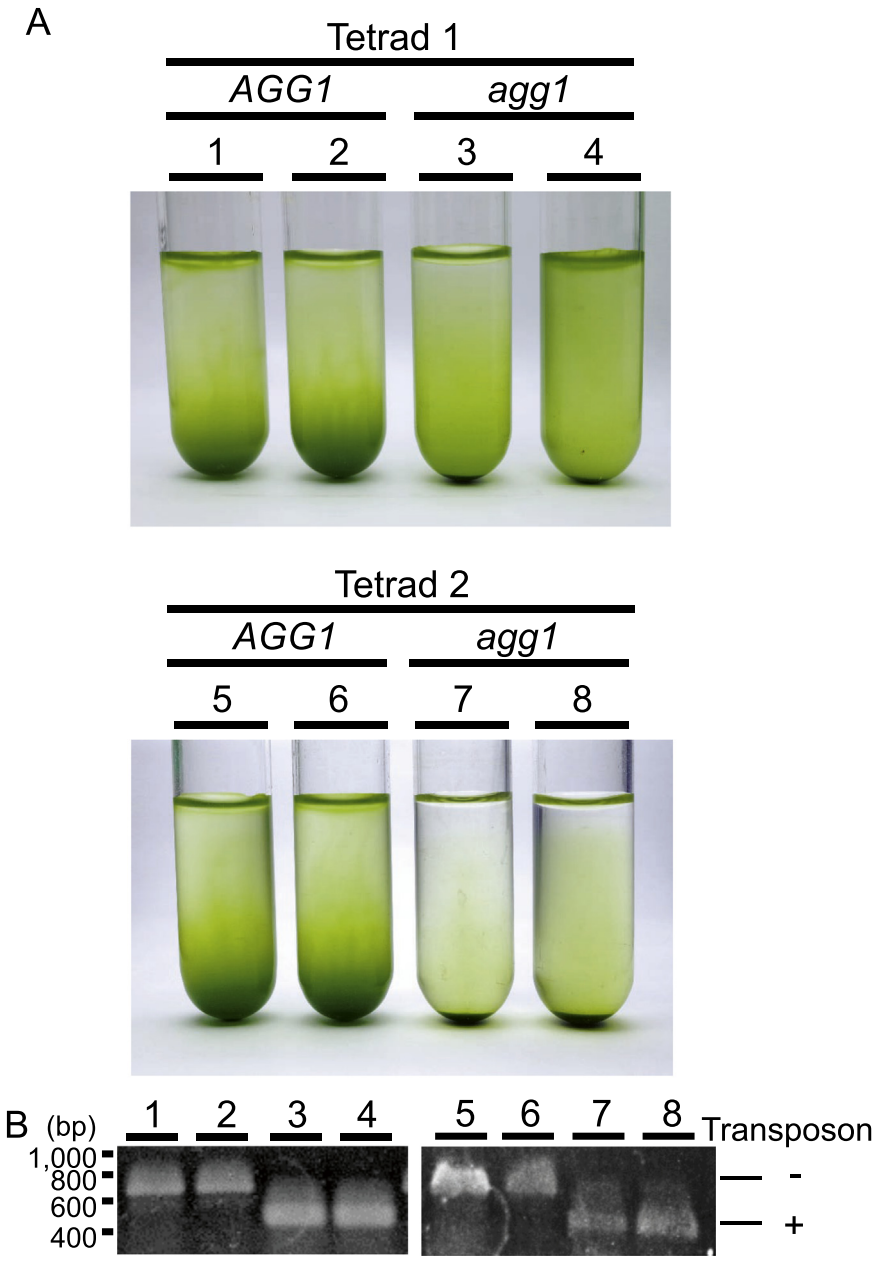

Fig. 2. The "agg" phenotype is closely correlated with the presence of a transposon. (A) Tube tests for the tetrads from the cross *agg1* (mt−) × CC-125 (mt+ wild type). Cell suspensions were photographed after being illuminated from the top for 30–45 min. Two progenies from each tetrad (3, 4, 7, 8) showed strong negative phototaxis and aggregated at the bottom of the tubes, whereas the other two progenies showed more dispersed distribution. (B) PCR detection of the transposon insertion. The reaction mixture contained three primers (#1~#3 in Fig. 1A). A 449-bp product is amplified with #1 and #3 when the transposon is present whereas a 674 bp product is amplified with #2 and #3 when it is not present. The transposon insertion was always in the progenies showing the "agg" phenotype.

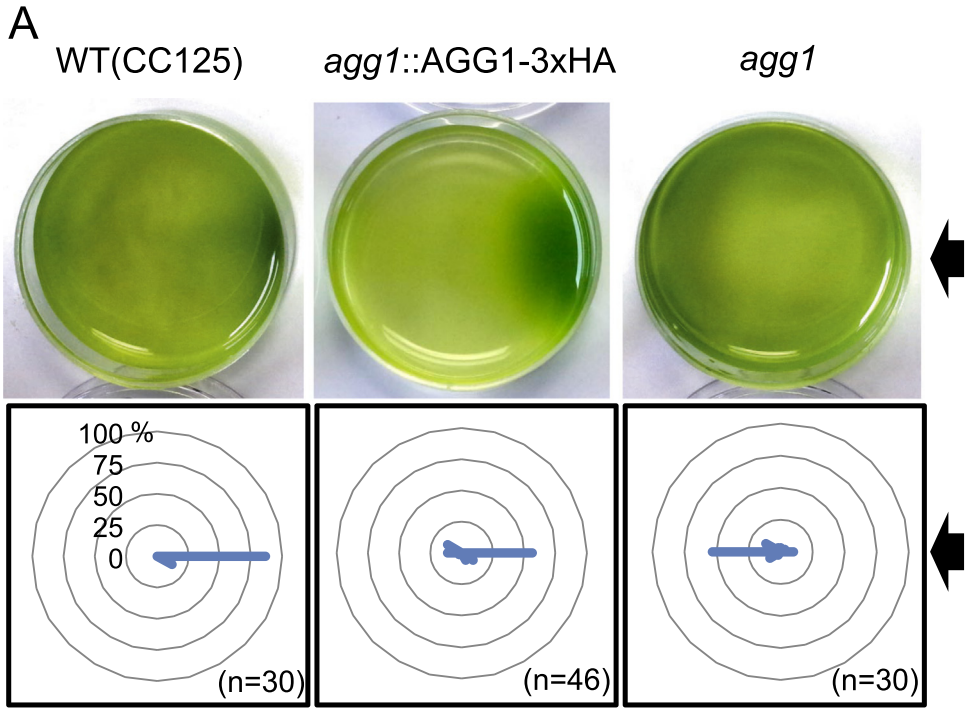

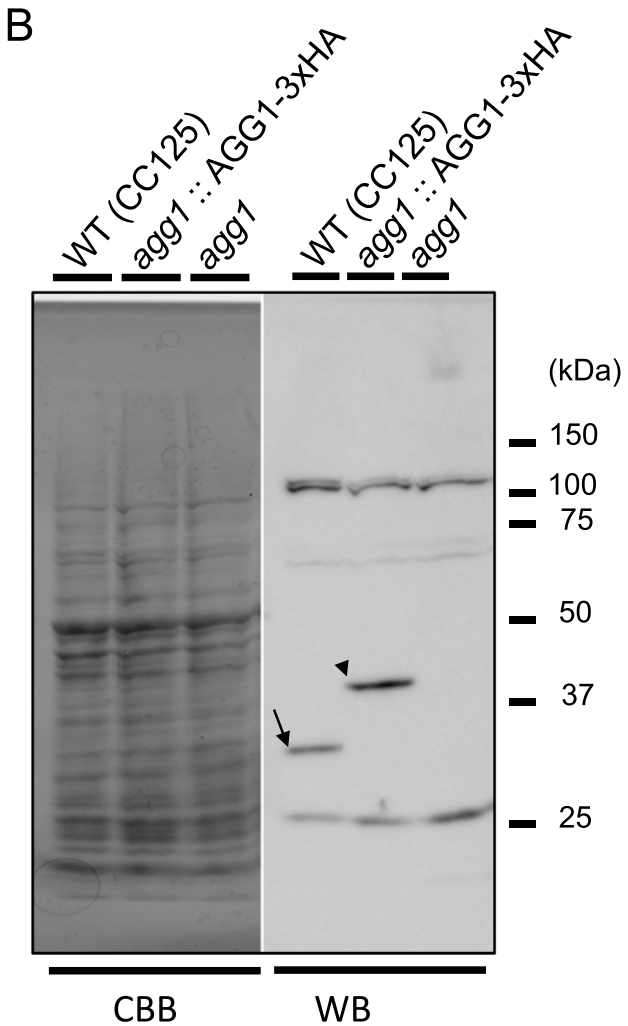

Fig. 3. AGG1-3 × HA rescues negative phototaxis in the *agg1* mutant. (A) (Top panels) Cell suspensions in Petri dishes were photographed after illumination from the right side for 10 min. CC125 (wild type) and *agg1* cells showed positive and negative phototaxis, respectively. The *agg1* cells expressing AGG1-3 × HA cells showed positive phototaxis. (Bottom panels). Polar histograms representing the percentage of cells moving in a particular direction (one of 12 bins of 30°) in a 1.5-s time window after 15 s of illumination from the right. (B) Western blot analysis against whole cell lysates (10 μg/lane). (Left) Proteins separated by SDS-PAGE were transferred to a PVDF membrane and stained with CBB. (Right) Anti-AGG1 antiserum detected both endogenous (35.8 kDa; arrow) and 3 × HA-tagged AGG1 (40.6 kDa; arrowhead). The bands near the 100 kDa and 25 kDa markers are likely non-specific.

The gene product of Cre13.g590400 is predicted to be a novel 317-amino-acid protein containing a Fibronectin type III domain and a CHORD-Sgt1(CS) domain (Fig. 1B). The Fibronectin type III domain has been found in a variety of proteins and does not suggest specific protein functions. The CS domain is the core of NudC, a protein associated with dynein and involved in nuclear migration; because of this, Cre13.g590400 has been annotated as a NudC-like protein (33% identical to murine NudC) [20,21].

3.2. Correlation between the loss of Cre13.g590400 and negative phototaxis

To determine whether Cre13.g590400 is in fact the causal gene of *agg1*, we examined the correlation between the presence of the transposon at the 5′ UTR of Cre13.g590400 and the phototactic behavior of the cell. We assayed tetrads from the *agg1* × CC-125 cross for the sign of phototaxis either by a "test-tube assay" (Materials and Methods), or by visual inspection under the microscope. In test-tube

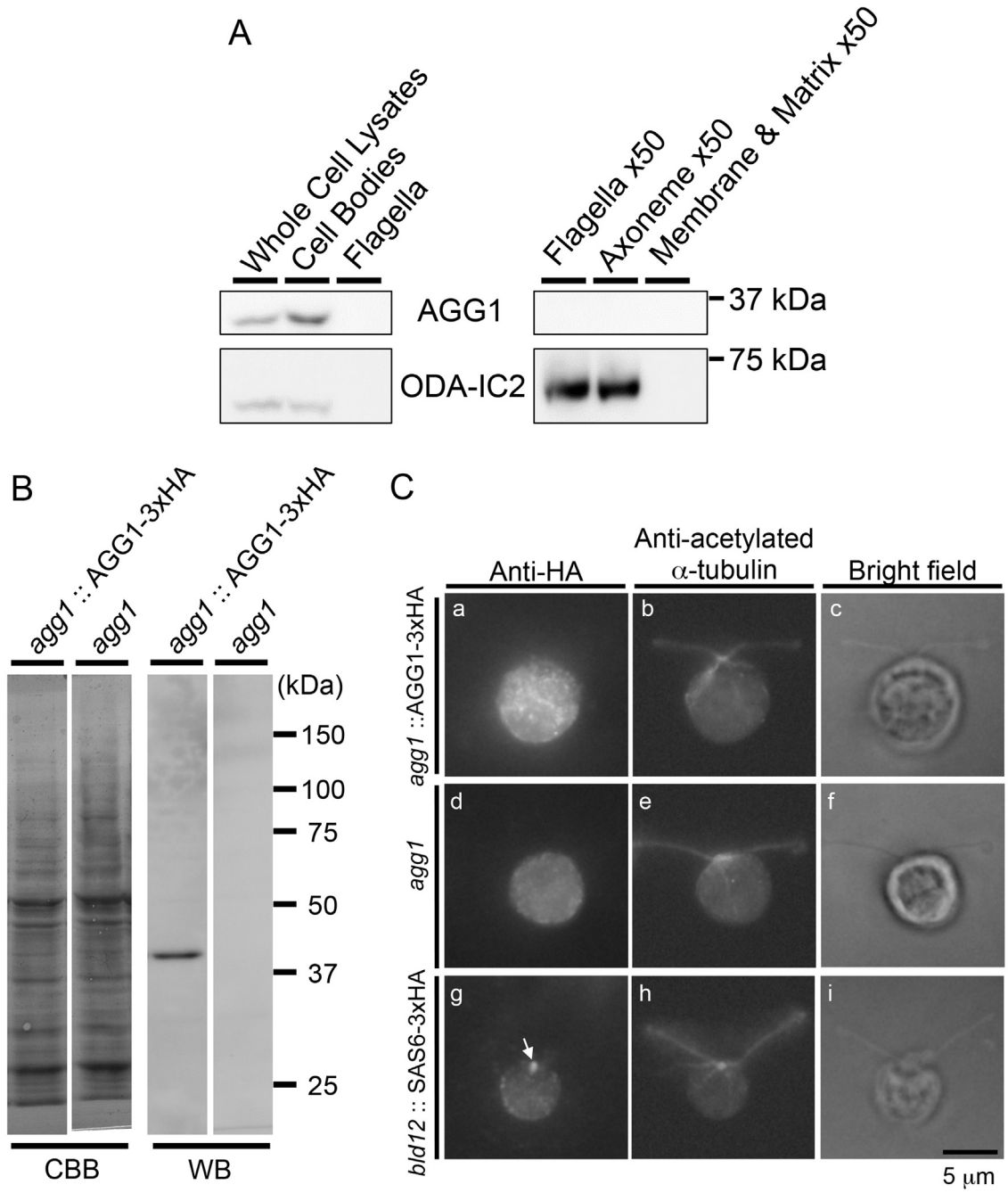

Fig. 4. AGG1 localizes to the cell body. (A) (Left) Western blot analysis against cellular fractions using anti-AGG1 (35.8 kDa) antibody and anti-ODA-IC2 (63.5 kDa) antibody (an outer arm dynein subunit antibody used as a flagellar axoneme marker). Samples obtained from the same amount of cells were loaded in the lanes of whole cell lysates, cell bodies and flagella. (Right) To examine whether a small amount of AGG1 localizes to flagella, a 50-fold higher concentration of flagella, axonemes, and membrane and matrix fraction were loaded; however, no bands were detected. (B) Western blot analysis using anti-HA antibody against whole cell lysates (10 μg/lane). (Left) Proteins separated by SDS-PAGE were transferred to a PVDF membrane and stained with CBB. (Right) Anti-HA antibody detected a single band of 3 × HA-tagged AGG1 (40.6 kDa) in the transformant. (C) Immunofluorescence microscopy to localize AGG1. (a–c) Typical images of *agg1*::AGG1-3 × HA, (d–f) *agg1* and (g–i) *bld12*::CrSAS6-3 × HA (a strain expressing an HA-tagged basal-body protein, used as positive control for HA-tag detection) treated with anti-HA antibody (a, d and g) or anti-acetylated α-tubulin antibody (b, e and h) are shown. Anti-HA antibody detected spots in the cell, not flagella, of *agg1*::AGG1-3 × HA (a, b), suggesting localization to the cell body. A spot in CrSAS-6-3 × HA represents basal bodies (g; arrow) [29].

assays, negatively phototactic cells tend to aggregate at the test tube bottom in response to the room light ("agg" phenotype) (Fig. 2A). In 80 tetrads (320 progenies) examined, progenies with opposite phototactic signs were always segregated 2:2, and the two progenies displaying negative phototaxis always contained the inserted transposon, as detected by PCR (Fig. 2B).

The segregation indicates that the transposon insertion in the Cre13.g590400 gene of *agg1* blocks its expression and cause negative phototaxis. To examine this possibility, we introduced Cre13.g590400 cDNA in an expression vector into the *agg1* mutant. As expected, the transformed cells expressing the Cre13.g590400 protein tagged with 3 × HA showed positive phototaxis under conditions where the *agg1* mutant showed negative phototaxis (Fig. 3A).

3.3. AGG1 is absent from agg1 cells

To detect the AGG1 protein (the product of the Cre13.g590400 gene, GenBank accession#: XP_001692941) in the cell, we raised antiserum against bacterially expressed protein. Western blot analysis of whole cell extract using the affinity-purified antiserum detected a band with the expected molecular mass of AGG1 (35.8 kDa) in wild type, and a band expected for 3 × HA-tagged AGG1 (40.6 kDa) in the transformant, but no bands in the *agg1* mutant (Fig. 3B). From these results, we concluded that Cre13.g590400 is the causal gene of the *agg1* mutation.

3.4. AGG1 is localized in the cell body

Western blot analysis of fractions from wild type cells indicated that AGG1 localizes to the cell body (Fig. 4A). Consistent with this observation, immunofluorescence images of the *agg1*::AGG1-3 × HA transformant using an anti-HA antibody, which detects only AGG1-3 × HA in western blotting, showed that AGG1 is present as small particles in the cell body (Fig. 4B and C). The signal did not appear to be concentrated at the eyespot or basal body. TargetP (http://www.cbs.dtu.dk/services/TargetP/), an analytical tool to predict the subcellular localization of eukaryotic proteins, suggests that AGG1 has a plant-type mitochondrial targeting peptide (mTP score=0.810) [22]. However, we have thus far been unable to detect mitochondrial localization of AGG1. Further studies are necessary to determine its subcellular localization.

4. Discussion

In this study, we identified the causal gene of the *agg1* mutation, which is carried by CC-124, a widely used wild-type strain of *C. reinhardtii*. In the *agg1* mutant, a transposon, TOC1, is inserted in the 5′ UTR of the Cre13.g590400 gene and blocks the expression of a 317 amino-acid polypeptide (AGG1) that localizes to the cell body. As stated in Introduction, *agg1* mutation may well be distributed among many kinds of *C. reinhardtii* mutants used in various research fields. Identification of the *agg1* gene sequence must be useful for detection and elimination of the *agg1* mutation from those mutants.

How does *agg1* display strong negative phototaxis? Detailed analyses of wild-type and *agg1* flagellar movements revealed that, in wild-type cells, the *trans*-flagellum (the one farthest from the eyespot) beats stronger than the *cis*-flagellum (the one nearest to the eyespot) after photoreception, whereas in *agg1* cells, the *cis*-flagellum beats stronger than the *trans*-flagellum after photostimulation [23,24]. The beating balance between the *cis*- and *trans*-flagella has been shown to be regulated by submicromolar Ca^{2+} [25,26]. However, in vitro motility reactivation of demembranated cell models in Ca^{2+} buffers showed no significant difference in the Ca^{2+} sensitivity between wild-type and *agg1* flagellar axonemes [5]. Thus, it is unlikely that the loss of AGG1 in the cell body directly affects flagellar function. Recently, cAMP is also shown to affect the beating balance between two flagella in vitro [26]. AGG1 may modulate the signaling pathway in which photoreception causes a change in cellular signals, such as cAMP or Ca^{2+} concentrations.

The properties of AGG1, including the function of Fibronectin type III and CS-domains, remain to be clarified. The CS-domain is known to be involved in a dynein-regulating protein NudC and *Chlamydomonas* has a NudC-like protein that regulates axonemal dyneins. However, it is unlikely that AGG1 is involved in dynein regulation since it is localized in the cell body and *Chlamydomonas* has no cytoplasmic dynein functioning in the cell body. BLAST search suggests that *Volvox carteri* and *Gonium pectorale* have AGG1 homologs, Vocar20015120m.g (XP_002949933.1) (62.1% similarity) and GPECTOR_33g581 (KXZ47699.1) (76.8% similarity), which also have Fibronectin type III- and CS-domains. It is interesting to note that these two organisms are colonial algae and may not need to regulate the beating balance of two flagella [27,28]. This feature also suggests that AGG1 is not directly involved in the regulation of flagellar beating, although it should be tested by determination of AGG1 localization in these algae or by knockdown/out experiments.

A previous study showed that the lack of *AGG2* or *AGG3* gene products also results in the "agg" phenotype [24]. AGG2 is a membrane protein that localizes to the proximal flagellar region, and AGG3 is a flavodoxin that localizes to the flagellar matrix. These proteins interact with each other and are suggested to function in a pathway that also involves AGG1 [24]. However, our results clearly showed that the localization of AGG1 differs from that of AGG2 or AGG3. *Volvox carteri* has multiple AGG2 homologs Vocar.0001s1693.1 (XP_002951946.1), Vocar.0001s1548.1 (XP_002947691.1), Vocar.0017s0113.1 (XP_002953333.1), and Vocar.0017s0112.1 (XP_002953334.1), and an AGG3 homolog Vocar.0028s0169.1 (XP_002947514.1). *Gonium pectorale* has an AGG2 homolog GPECTOR_15g310 (KXZ50626.1) and an AGG3 homolog GPECTPR_60g718 (KXZ44941.1). Intriguingly, AGG2 is conserved in plants (e.g. *Oryza sativa* indica group EAY92439.1; *Medicago truncatula* AFK38344.1) and so is AGG3 (e.g. *Citrus clementine* XP_006452110.1; *Brassica oleracea* var. oleracea XP_013625297.1). Because these plants do not have AGG1 homologs, this also indicates that AGG1 functions in a different pathway from that involves AGG2 and AGG3. For determination of the functional relationship between AGG1, AGG2 and AGG3, identification of the structural basis for the punctate localization of AGG1 and analysis of light-induced changes in cytoplasmic factors in *agg1*∼*agg3* mutants should be important future challenges.

Acknowledgments

We thank Dr. Tatsuya Kitazume, Ms. Hisayo Asao (NIBB), and Ms. Mishio Toh (Univ. Tokyo) for Illumina sequencing, Ms. Naomi Miyamoto (Hosei Univ.) for linkage mapping, Dr. Toru Hisabori (Tokyo Tech) for fruitful discussion, and Dr. Ritsu Kamiya (Gakushuin Univ.) for critical reading of this manuscript. This work was supported by JSPS KAKENHI Grant numbers 25291058, 26650093, 15H01206, and 15H01314 to KW, National Institute for Basic Biology Collaborative Research Program 14-733 to KW and Network Joint Research Center for Materials and Devices 2015298 to MH.

Appendix A. Transparency document

Transparency document associated with this article can be found in the online version at http://dx.doi.org/10.1016/j.bbrep.2016.07.016.

References

[1] E.H. Harris, The Chlamydomonas sourcebook, 2nd ed., 2009.
[2] T. Proschold, E.H. Harris, A.W. Coleman, Portrait of a species: *Chlamydomonas reinhardtii*, Genetics 170 (2005) 1601–1610.
[3] R.D. Smyth, W.T. Ebersold, Genetic investigation of a negatively phototactic strain of *Chlamydomonas reinhardtii*, Genet. Res. 46 (1985) 133–148.
[4] M. Boonyareth, J. Saranak, D. Pinthong, Y. Sanvarinda, K.W. Foster, Roles of cyclic AMP in regulation of phototaxis in *Chlamydomonas reinhardtii*, Biologia (2009) 1058–1065.
[5] K. Wakabayashi, Y. Misawa, S. Mochiji, R. Kamiya, Reduction-oxidation poise regulates the sign of phototaxis in *Chlamydomonas reinhardtii*, Proc. Natl. Acad. Sci. USA (2011) 11280–11284.
[6] T. Kondo, C.H. Johnson, J.W. Hastings, Action spectrum for resetting the circadian phototaxis rhythm in the CW15 strain of Chlamydomonas 1. Cells in darkness, Plant Physiol. (1991) 197–205.
[7] D.S. Gorman, R.P. Levine, Cytochrome f and plastocyanin: their sequence in the photosynthetic electron transport chain of *Chlamydomonas reinhardii*, Proc. Natl. Acad. Sci. USA 54 (1965) 1665–1669.
[8] Y. Nakazawa, M. Hiraki, R. Kamiya, M. Hirono, SAS-6 is a cartwheel protein that establishes the 9-fold symmetry of the centriole, Curr. Biol. 17 (2007) 2169–2174.
[9] C.H. Gross, L.P.W. Ranum, P.A. Lefebvre, Extensive restriction fragment length polymorphisms in a new isolate of *Chlamydomonas-reinhardtii*, Curr. Genet. 13 (1988) 503–508.
[10] P. Kathir, M. LaVoie, W.J. Brazelton, N.A. Haas, P.A. Lefebvre, C.D. Silflow, Molecular map of the *Chlamydomonas reinhardtii* nuclear genome, Eukaryot. Cell 2 (2003) 362–379.
[11] G. Shiratsuchi, R. Kamiya, M. Hirono, Scaffolding function of the Chlamydomonas procentriole protein CRC70, a member of the conserved Cep70 family, J. Cell Sci. 124 (2011) 2964–2975.
[12] N. Fischer, J.-D. Rochaix, The flanking regions of PsaD drive efficient gene expression in the nucleus of the green alga *Chlamydomonas reinhardtii*, Mol. Genet. Genom. 265 (2001) 888–894.
[13] I. Sizova, M. Fuhrmann, P. Hegemann, A Streptomyces rimosus aphVIII gene coding for a new type phosphotransferase provides stable antibiotic resistance to *Chlamydomonas reinhardtii*, Gene 277 (2001) 221–229.
[14] T. Yamano, H. Iguchi, H. Fukuzawa, Rapid transformation of *Chlamydomonas reinhardtii* without cell-wall removal, J. Biosci. Bioeng. 115 (2013) 691–694.
[15] M.A. Sanders, J.L. Salisbury, Immunofluorescence microscopy of cilia and flagella, Methods Cell Biol. 47 (1995) 163–169.
[16] K. Wakabayashi, S. Takada, G.B. Witman, R. Kamiya, Transport and arrangement of the outer-dynein-arm docking complex in the flagella of Chlamydomonas mutants that lack outer dynein arms, Cell Motil. Cytoskelet. 48 (2001) 277–286.
[17] A. Day, M. Schirmerrahire, M.R. Kuchka, S.P. Mayfield, J.D. Rochaix, A transposon with an unusual arrangement of long terminal repeats in the green-alga *Chlamydomonas-reinhardtii*, Embo J. 7 (1988) 1917–1927.
[18] R.T. Poulter, M.I. Butler, Tyrosine recombinase retrotransposons and transposons, Microbiol. Spectr. 3 (2015), MDNA3-0036-2014.
[19] S.D. Gallaher, S.T. Fitz-Gibbon, A.G. Glaesener, M. Pellegrini, S.S. Merchant, Chlamydomonas genome resource for laboratory strains reveals a mosaic of sequence variation, identifies true strain histories, and enables strain-specific studies, Plant Cell 27 (2015) 2335–2352.
[20] Y.T. Lee, J. Jacob, W. Michowski, M. Nowotny, J. Kuznicki, W.J. Chazin, Human Sgt1 binds HSP90 through the CHORD-Sgt1 domain and not the tetratricopeptide repeat domain, J. Biol. Chem. 279 (2004) 16511–16517.
[21] P. Bork, A.K. Downing, B. Kieffer, I.D. Campbell, Structure and distribution of modules in extracellular proteins, Q. Rev. Biophys. 29 (1996) 119–167.
[22] O. Emanuelsson, H. Nielsen, S. Brunak, G. von Heijne, Predicting subcellular localization of proteins based on their N-terminal amino acid sequence, J. Mol. Biol. 300 (2000) 1005–1016.
[23] U. Ruffer, W. Nultsch, Flagellar coordination in Chlamydomonas cells held on micropipettes, Cell Motil. Cytoskelet. 41 (1998) 297–307.
[24] C. Iomini, L. Li, W. Mo, S.K. Dutcher, G. Piperno, Two flagellar genes, AGG2 and AGG3, mediate orientation to light in Chlamydomonas, Curr. Biol. 16 (2006) 1147–1153.
[25] R. Kamiya, G.B. Witman, Submicromolar levels of calcium control the balance of beating between the two flagella in demembranated models of Chlamydomonas, J. Cell Biol. 98 (1984) 97–107.
[26] Y. Saegusa, K. Yoshimura, cAMP controls the balance of the propulsive forces generated by the two flagella of Chlamydomonas, Cytoskeleton 72 (2015) 412–421.
[27] N. Ueki, S. Matsunaga, I. Inouye, A. Hallmann, How 5000 independent rowers coordinate their strokes in order to row into the sunlight: phototaxis in the multicellular green alga Volvox, BMC Biol. 8 (2010) 103.
[28] H.J. Hoops, Motility in the colonial and multicellular Volvocales: structure, function, and evolution, Protoplasma 199 (1997) 99–112.
[29] M. van Breugel, M. Hirono, A. Andreeva, H.A. Yanagisawa, S. Yamaguchi, Y. Nakazawa, N. Morgner, M. Petrovich, I.O. Ebong, C.V. Robinson, C. M. Johnson, D. Veprintsev, B. Zuber, Structures of SAS-6 suggest its organization in centrioles, Science 331 (2011) 1196–1199.